

# The role of coordinating anions in the supporting electrolyte during the electrocatalytic oxidation of glycerol on Pt electrodes

Gabriel Melle<sup>a</sup>, Juan M. Feliu<sup>a,\*</sup>, Enrique Herrero<sup>a,\*</sup>, Germano Tremiliosi-Filho<sup>b</sup>, Vinicius Del Colle<sup>c</sup>, Camilo A. Angelucci<sup>d,\*</sup>

<sup>a</sup> Instituto de Electroquímica, Universidad de Alicante, Apdo. 99, E-03080 Alicante, Spain

<sup>b</sup> Institute of Chemistry of São Carlos, University of São Paulo, Av. Trabalhador São Carlense, 400, 13566-590 São Carlos, São Paulo, Brazil

<sup>c</sup> Aeronautics Technological Institute, Chemistry Department, Praça Marechal Eduardo Gomes, 50 Vila das Acácias, 12228-900 São José dos Campos, São Paulo, Brazil

<sup>d</sup> Federal University of ABC, Center for Natural and Human Sciences, Av. dos Estados, 5001, 09210-580 Santo André, São Paulo, Brazil

## ARTICLE INFO

### Keywords:

Glycerol electro-oxidation reaction  
Pt surface  
Cyclic voltammetry  
Potential oscillations  
*In situ* FTIR  
Anions effect

## ABSTRACT

This research explores the glycerol electrooxidation reaction (GEOR) on a platinum electrode, with a special emphasis on the role of the chemical properties of the anion present in the electrolyte composition. Essential knowledge of the mechanism and dynamics of glycerol electrooxidation is obtained through comprehensive studies that involve *in situ* FTIR measurements and the analysis of electrochemically oscillatory responses. This study addresses on the complex interplay between anion adsorption strength and the GEOR, focusing on the differences in CO adsorption coverage, which is the main strongly adsorbed intermediate. The anion adsorption strength, with the order  $\text{HClO}_4 < \text{H}_2\text{SO}_4 < \text{H}_3\text{PO}_4$ , affects significantly not only the CO coverage on the platinum surface but also the overall glycerol electrooxidation rate. The observed differences in the electroactivity are attributed to competitive adsorption phenomena, in which specific coordinated ions have greater adsorption capabilities than perchlorate ions. These findings highlight the critical relevance of designing and optimizing electrocatalysts for glycerol electrooxidation and related processes with careful consideration of the electrolyte composition, notably the anion.

## 1. Introduction

Rational design and optimization of electrocatalytic processes require a thorough understanding of the delicate interaction between electrode materials, reagents, and surrounding electrolyte species. Among the different parameters influencing electrocatalytic processes, the electrolyte anions emerge as a significant driver in determining reaction kinetics and mechanisms. The influence of the electrolyte anions on the electrochemical oxidation of different small organic molecules and electrode materials has been reported as a determining factor [1–3]. The selection of electrolyte anions affects not only the overall electrochemical performance but also the selectivity, stability, and efficiency of the catalytic process [4–6]. This pivotal role of anions in electrocatalysis stems from their ability to modulate surface adsorption processes, alter charge transfer dynamics, and facilitate specific reaction pathways [7–9].

In the context of electrochemical oxidation reactions, platinum (Pt) electrodes have attracted substantial interest due to their exceptional

catalytic properties and compatibility with numerous organic molecules. The electrooxidation of glycerol, a polyol of increasing significance in renewable energy and chemical industries, presents a platform for investigating the intricate interplay between anions and electrode interfaces. An important finding from a recent study is that glycerol may be effectively converted into molecules with added value such as glyceraldehyde, glyceric acid, dihydroxyacetone, tartaric acid, oxalic acid, and formic acid [10–12]. Additionally, glycerol electro-oxidation takes place at far lower overall potentials with relatively high oxidation rates on Pt, Au, and Pd [13] than oxygen evolution reaction, so it can be used as an anode reaction in the production of hydrogen from water. When studying this oxidation reaction, the adsorption of anions onto Pt surfaces introduces complexities that extend beyond conventional electrochemical paradigms, manifested as dynamic instabilities and intricate reaction networks. Thus, to understand the actual electrode performance scenario, it is essential to learn about the various aspects involved during the specific adsorption of different anions on the metal. In the electrochemical processes, anions adsorption on the catalyst

\* Corresponding authors.

E-mail addresses: [juan.feliu@ua.es](mailto:juan.feliu@ua.es) (J.M. Feliu), [herrero@ua.es](mailto:herrero@ua.es) (E. Herrero), [camilo.angelucci@ufabc.edu.br](mailto:camilo.angelucci@ufabc.edu.br) (C.A. Angelucci).

<https://doi.org/10.1016/j.electacta.2024.144698>

Received 27 May 2024; Received in revised form 4 July 2024; Accepted 8 July 2024

Available online 9 July 2024

0013-4686/© 2024 The Authors. Published by Elsevier Ltd. This is an open access article under the CC BY license (<http://creativecommons.org/licenses/by/4.0/>).

surface can block active sites, reducing the catalytic activity and impacting the kinetics of reactions. Therefore, understanding and controlling anion adsorption is crucial for improving the performance of fuel cell catalysts.

Studies related to anion adsorption such as sulfate, perchlorate, dihydrogen phosphate, chlorine, and hydroxyl, and how these anions affect the oxidation of organic molecules have been an object of investigation for a long time. Iwasita et al. [14] studying methanol electro-oxidation observed that sulfate adsorption impacts the oxidation mechanism. Thus, CO<sub>2</sub> formation is inhibited in the presence of this anion, and the amount of CO<sub>2</sub> produced in perchlorate solutions is ca. 20 higher than in sulfuric acid solutions. Concerning the anion effect on the ethanol electro-oxidation reaction on Pt(111)/Rh/Sn surfaces, Paulino et al. [15] compared the anion effect by in situ FTIR. Also, in this case, the mechanism was altered due to the nature of the electrolyte anion. In perchloric and sulfuric acid electrolytes were observed the formation of acetaldehyde, acetic acid, and CO<sub>2</sub>; while phosphate anion exerts a strong adsorption and competes by active sites with ethanol favoring the acetaldehyde and CO<sub>2</sub> production route. Recently, Del Colle et al. [16], using Pt single crystals demonstrated that an increase in sulfate concentration impacts negatively towards glycerol electro-oxidation, in this case, the current densities diminish drastically.

Another outstanding type of adsorption comes from water dissociation to yield adsorbed OH on the Pt surface. This process is responsible for promoting CO oxidation, and its occurrence may depend on the electrolyte used to study the reaction [1,17,18]. Studies of the role of anion adsorption towards CO oxidation have demonstrated that species like sulfate and chlorine anions compete for Pt sites and prevent OH formation, which is required to oxidize adsorbed CO. As a result, the peak of CO oxidation is displaced to more positive potentials and the current densities diminish drastically [1].

Therefore, anion adsorption affects the electrochemical responses of different processes, namely, the electrocatalytic reaction. In this paper, we will report for the first time the influence of three distinct electrolyte anions ClO<sub>4</sub><sup>-</sup>, SO<sub>4</sub><sup>2-</sup>, and HPO<sub>4</sub><sup>2-</sup> on the glycerol electrooxidation reaction at Pt electrode interfaces. By employing a combination of dynamic instability analysis and in situ FTIR, the intricate role of anions in shaping the glycerol electrooxidation mechanism and kinetics is unraveled. The dynamic nature of anion adsorption and its subsequent impact on reaction pathways provide insights into the mechanism of glycerol oxidation on Pt electrodes.

## 2. Experimental

The electrochemical experiments were conducted in a conventional three-electrode cell with an atmosphere of argon gas (99.999 %) and temperature was maintained at 25 °C using a thermostatic bath. The working electrode (WE) was either a smooth polycrystalline Pt sheet of 1.6 cm<sup>2</sup> of active area or a Pt disk with 0.78 cm<sup>2</sup> of active area (FTIR). and the counter-electrode (CE) was a Pt sheet. The reference electrode used in all experiments was the reversible hydrogen electrode (RHE). All potentials presented in this paper are referenced to the RHE, and the current was normalized by the electroactive area represented in current density (*j*)

The supporting electrolytes solutions were prepared with HClO<sub>4</sub> (ACS reagent, 70 %), H<sub>2</sub>SO<sub>4</sub> (Merck, 95–97 %), and H<sub>3</sub>PO<sub>4</sub> (ACS reagent, 70 %) with ultra-pure water (18.2 MΩ cm, Millipore), using an acid concentration of 1.0 mol L<sup>-1</sup>. All the electrochemical experiments were done under an argon atmosphere. A cyclic voltammogram (blank) was recorded to verify the cleanness of the systems (see Fig. SII).

Briefly, before the beginning of the glycerol electrooxidation studies, a cyclic voltammogram (blank) was recorded at 0.02 mV s<sup>-1</sup>, from 0.05 to 1.30 V (vs. RHE) to attest the cleanness of the systems (see Fig. SII). Thereafter glycerol (Sigma-Aldrich, >99 % GC) was added directly into the cell yielding a 0.5 mol L<sup>-1</sup> solution. After this procedure, 8 scans were recorded at a range of 0.05 to 1.30 V and a scan rate of 0.02 mV s<sup>-1</sup>.

The potentiostatic and potentiodynamic experiments, the electrodes were submitted to four voltammetric cycles in the glycerol solutions (0.5 mol L<sup>-1</sup>). Then a linear sweep at 0.01 V s<sup>-1</sup> in 1 mol L<sup>-1</sup> of HClO<sub>4</sub>, H<sub>2</sub>SO<sub>4</sub>, and H<sub>3</sub>PO<sub>4</sub> with four different external resistors (1.6, 3.2, 6.4, 9.6, 12.8 and 16.0 kΩ cm<sup>2</sup>) is performed and the current vs. potential curves obtained showed the contribution without and with ohmic drop correction ( $E = \varphi - iR$ ).

Spectroelectrochemical experiments were carried out with a VERTEX 70 V Bruker spectrometer equipped with an LN-MCT Mid detector. The spectra were computed from the average of 64 interferograms and the spectral resolution was set to 4 cm<sup>-1</sup>. The reference spectrum (R<sub>0</sub>) was collected at 0.05 V in the same experiment. A flat CaF<sub>2</sub> was used as the infrared window and the working electrode was pressed against this window, leaving a thin layer of electrolyte between the window and electrode. *In situ* FTIR data were collected simultaneously during successive potential steps of 0.05 V intervals. This procedure was carried out for two consecutive scans between 0.05 and 1.3 V. Positive and negative bands represent the loss and gain of species, respectively, at the sampling potential with respect to those present at the interface at the reference potential.

## 3. Results

The cyclic voltammetric profiles of glycerol electrooxidation on a Pt polycrystalline (Pt<sub>poly</sub>) electrode in the presence of the three studied acids are shown in Fig. 1. The current response of a linear potential sweep between 0.05 - 1.30 V is represented by the solid and dotted lines for positive and negative scan directions, respectively.

The typical voltammetric behavior of Pt<sub>poly</sub> electrode for GEOR presents two oxidation peaks at, approximately, 0.70 and 0.80 V (namely *peak 1* and *peak 2*), followed by a third oxidation process (*peak 3*), concurrent with platinum oxide formation, which starts at potentials higher than 1.1 V [19,20]. The primary characteristic feature of these CVs is the clear difference in the current density for the oxidation peaks, indicating the role of the anions during the GEOR, following the sequence: HPO<sub>4</sub><sup>2-</sup> < SO<sub>4</sub><sup>2-</sup> < ClO<sub>4</sub><sup>-</sup>. Otherwise, there is also a slight shift in the peak positions to higher potentials following the sequence: H<sub>3</sub>PO<sub>4</sub> (0.74 - 0.85 V), H<sub>2</sub>SO<sub>4</sub> (0.72 - 0.83 V), and HClO<sub>4</sub> (0.71 - 0.80 V).

Regarding the onset potential for glycerol oxidation, our data shows that the main difference is observed amongst the non-coordinate anion, namely Perchlorate, and the other two anions that are characterized to adsorb strongly (Sulfate and Phosphate). Although the differences are low (more details will be discussed in Fig. 4 with in situ FTIR data help). Considering the adsorption energy of the studied anions, the results observed during the positive sweep show that they are closely related: i. e., the higher the adsorption strength on Pt, the lower the electrocatalytic response [6,21,22].

In general, the rates of glycerol electrooxidation in perchloric acid solutions would exceed those observed in solutions containing anions with higher adsorption strengths. This phenomenon primarily arises from the competing adsorption of the reactant and anions at the electrode surface. While this explanation seems intuitive for the electro-oxidation of organic molecules on platinum surfaces, it involves several other considerations. Indeed, Herrero et al. [8] studying the electro-oxidation reaction of methanol on Pt(*hkl*) electrodes in different acids as electrolytes reported, that despite the dependence of the electrode surface orientation, the density current response an inverse dependence with the increase of the chemisorption strength of the anions in the supporting electrolyte.

In the example cited above, CO formation and adsorption are considered a key step in the electrooxidation mechanism of some small alcohols. For ethanol and formic acid oxidation, this trend is not consistently observed. This suggests that intermediate species formed during oxidation, or even the reactants themselves (such as formic acid), may also participate in the mechanism by competing for free surface sites along with the anions from the electrolyte [3–5]. Conversely, Melle

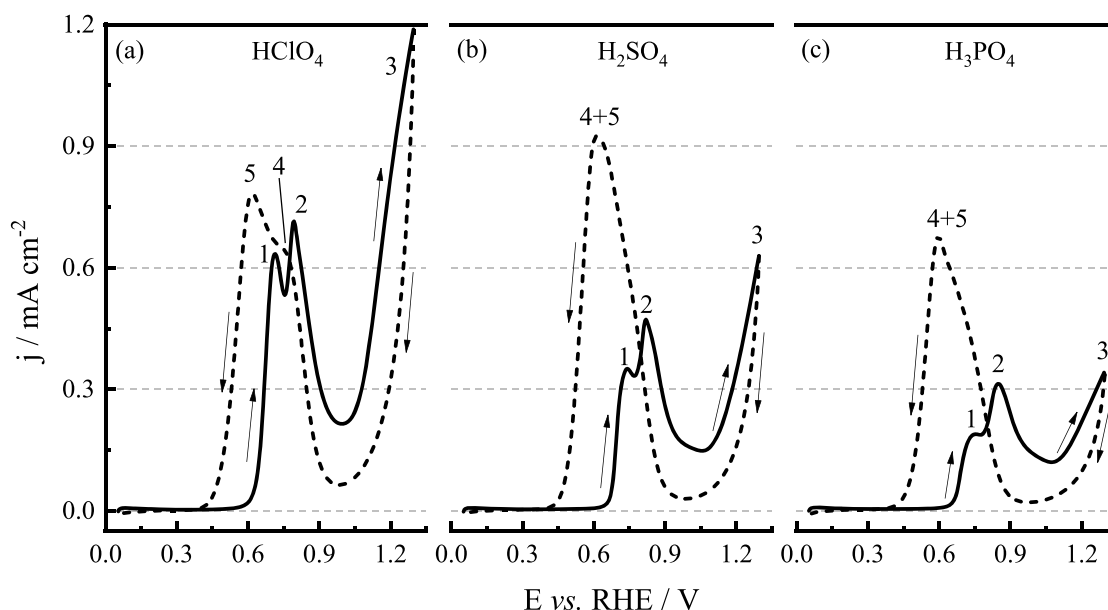


Fig. 1. Cyclic voltammograms for the Pt electrode in 0.5 mol L<sup>-1</sup> glycerol + 1.0 mol L<sup>-1</sup> (a) HClO<sub>4</sub> (b) H<sub>2</sub>SO<sub>4</sub> (c) H<sub>3</sub>PO<sub>4</sub>. Solid and dotted lines represent positive and negative scan directions, respectively.

et al. [23] demonstrated that CO surface poisoning does not result directly from the oxidation of glycerol, but rather from partially oxidized products like glyceraldehyde and glyceric acid. In this way, our findings can be understood by considering the modification in the energetic surface balance, which involves the formation and co-adsorption of hydroxyl groups (OH) with glycerol, its reactive partially oxidized products, and anions. This interplay dictates the overall adsorption processes and the electrooxidation reaction. Further discussion on this topic will be provided through in situ FTIR data, which offers deeper insights into the adsorption phenomena and surface interactions during the electrooxidation of glycerol.

After the scan reversal, the current decays due to the irreversible oxidation of the surface. However, as the potential is made more negative,  $E < 1.0$  V, the glycerol oxidation reaction resumes giving rise to a small shoulder at  $\sim 0.75$  V, denoted as peak 4, followed by a broad peak with a maximum centered at  $\sim 0.61$  V, denoted as peak 5 (Fig. 1). From that point, the current density response rapidly decreases and, at potentials below 0.40 V, the oxidation rates become negligible due to a lack of oxy-hydroxides species (OH<sub>ads</sub>) formation, and the surface is re-poisoning by the adsorption of intermediates from GEOR. It should be noted that, in the reverse scan, oxidation currents occur at a potential c. a. 0.2 V less positive than those observed in the positive scan direction. The differences in the offset of GEOR during the negative scan direction when compared to the onset observed in the positive scan are associated with the formation and surface coverage by the adsorption of CO and other strong adsorbed intermediates. This behavior has also been observed in the oxidation processes of various small organic molecules, including formaldehyde [24], formic acid [25], methanol [26], ethylene glycol [27], ethanol [28] e glycerol [29]. Below 0.6 V, the rates for the oxidation adsorbed CO diminish significantly and CO accumulates on the surface leading to the progressive diminution of currents in the negative scan direction.

The differences in the voltammogram during the negative scan direction reveal the significant role of anions in the electrochemical environment. To gain a deeper understanding of the effect of the anions in GEOR, it is essential to determine the contribution of the distinct processes shaping the electrochemical response observed in Fig. 1. For this purpose, a deconvolution approach to separate the two independent processes, (peak 4 and 5), which together form the entire peak has been proposed [30]. The reverse scan curves recorded for each studied anion

were subjected to mathematical deconvolution, resulting in two distinct symmetric Gaussian peaks with a linear background. The results obtained using the deconvolution methodology are presented in Fig. 2A, where the two Gaussian curves are shown in different colors and the blue line represents the sum of these curves. The integration of the curves allows us to determine the oxidation charges associated with each peak, which were then analyzed as a function of the electrolyte composition, as presented in Fig. 2B. As can be observed, the overall influence of the anions, represented by the sum of the two peak areas, exhibits a clear trend with the adsorption strength: a higher adsorption strength corresponds to a lower electrooxidation rate. However, upon closer analysis of the contribution of each process, it becomes evident that peak 5 is primarily responsible for the observed trend, as the electrochemical charge for peak 4 remains relatively constant regardless of the nature of the anion.

This finding suggests that differences in adsorption strength predominantly affect peak A behavior, or more precisely, the deactivation of the overall electrooxidation process. Conversely, peak 4 can be associated with the reactivation of the GEOR during the reverse scan. In this way, the behavior of peak 4 can be linked to the reduction of oxide-like species formed at high potentials, which is essential to enable the adsorption of glycerol molecules on platinum-free sites and their subsequent oxidation. Remarkably, our findings suggest that the formation and posterior reduction of platinum surface oxides are not significantly influenced by the nature of the anion in the electrolyte, within the potential range considered (0.92 - 0.70 V). (See Fig.S1)

In the second stage of the oxidative process, as the potential becomes more negative, the amount of surface oxides decreases and a distinctive behavior marked by peak A emerges, closely tied to the electrolyte anions adsorption strength. The concurrent adsorption of anions with the intermediate species generated throughout the glycerol oxidation process leads to a sequential decrease in the oxidation charge which follows the adsorption strength of the studied anions: perchlorate < sulfate < phosphate [31]. To learn more about the observed events, in-situ FTIR spectroscopy was used to investigate the role of anions during the electrochemical oxidation of glycerol. The findings, which are presented below, will shed light on the nature of these complex processes

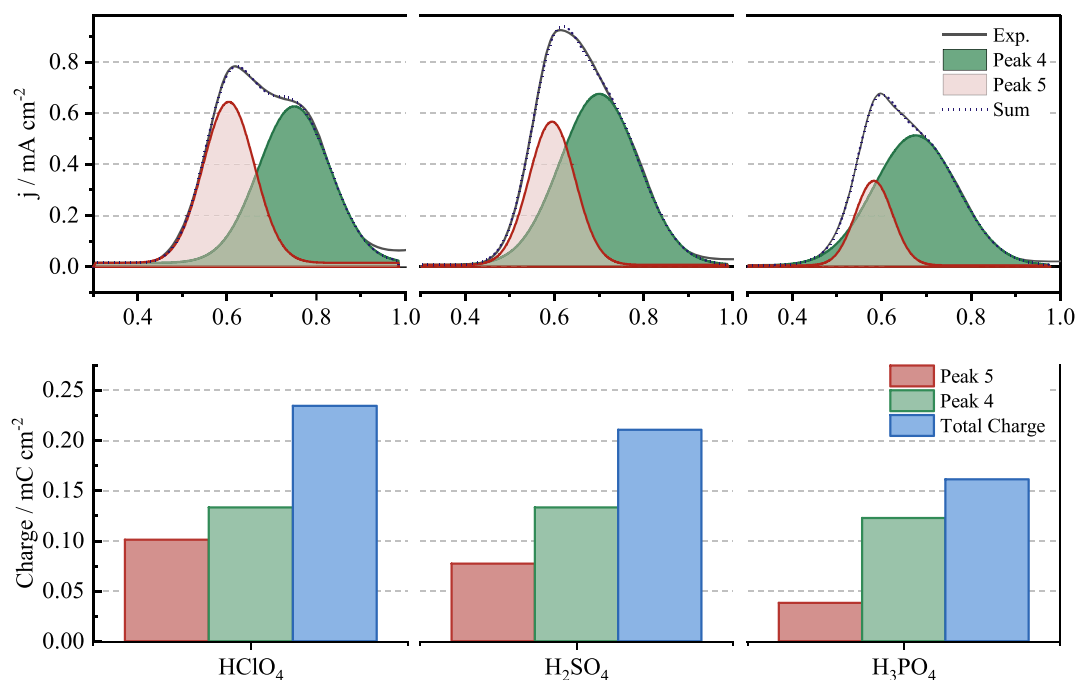


**Fig. 2.** Deconvolution of the peak and shoulder observed in the negative scan, corresponding to Peaks IV and V displayed in Fig. 1 for the glycerol electrooxidation on platinum in (a1) HClO<sub>4</sub>, (a2) H<sub>2</sub>SO<sub>4</sub>, or (a3) H<sub>3</sub>PO<sub>4</sub> electrolytes.

### 3.1. In situ FTIR studies of the glycerol electrooxidation in different electrolytes

A set of in situ FTIR spectra were collected during a potential-step sweep perturbation. The reference spectra were recorded at 0.05 V. The FTIR spectra in the presence of the three different anions are present in Fig. 3. Only the FTIR spectrum series of the second potential-step sweep is displayed as a representation of the steady behavior over the subsequent sweeps. The FTIR results for the first potential-step sweep are shown in the Support Information - Fig. S2.

Firstly, it should be mentioned that the signal response of the in situ FTIR technique is notably influenced by the thin layer's thickness and is intrinsically related to these particular experimental conditions. In this case, we performed two consecutive scans. During the second scan, the surface of the electrode was already modified by CO, and other adsorbates formed in the first scan. Additionally, products generated during the first scan, including partially oxidized soluble species, remained dissolved in the thin layer, which could potentially influence the spectral features observed in the second scan.

In this sense, irrespective of the anion present in the electrochemical medium, the potential-dependent FTIR spectra for glycerol electrooxidation reveal no significant qualitative variations among the studied anions. Consistent band features emerge in the recorded spectra at wavenumbers 2340, 2050, 1640, 1731, and 1240 cm<sup>-1</sup>. However, the broadband centered at 1640 cm<sup>-1</sup>, associated with water bending, should be analyzed carefully since its orientation, whether positive or negative, results from the water migration into or out of the thin layer configuration. The potential behavior of the IR bands reported here, as well as product assignments, agree with previous results publication [10,32,33].

The band centered at 2343 cm<sup>-1</sup> corresponds to the asymmetric stretching of CO<sub>2</sub> formed from the total oxidation of glycerol. The presence of adsorbed linear adsorbed CO (CO<sub>L</sub>) results in the appearance of a band at ca. 2050 cm<sup>-1</sup>, whose position depends on the electrode potential. The band at 1740 cm<sup>-1</sup> is assigned to the stretching vibration of the C=O group corresponding to carbonyl-containing compounds, as aldehyde or ketone and/or carboxylic species in solution, and the 1240 cm<sup>-1</sup> feature is attributed to C-O bond in carboxylic group. The

combination of these two bands suggests that the primary products resulting from glycerol electrooxidation (GEOR) are carboxylic acids, including dihydroxyacetone (DHA), glyceric acid (GA), glycolic acid (GCA), glyoxylic acid (GOA), oxalic acid (OA), tartronic acid (TA), and formic acid (FA). In the case of the GEOR on Pt, the literature indicates that the prevailing scenario is characterized by its incomplete oxidation [34–36]. The absence of significant differences among the three studied media, despite the difference in the strength of surface adsorption, can be related as a consequence of the formation of carboxylic acids as final products.

The FTIR results suggest the glycerol mechanism reaction seems to not be affected by the different anions present in the electrolyte, but only its kinetics. In all the electrolyte anions studied, the incomplete oxidation of glycerol to carboxylic acids and the cleavage of the C–C bond to form CO and finally its complete oxidation to CO<sub>2</sub> is observed. As explored in the subsequent section, the formation of CO plays a pivotal role in comprehending the potential instabilities that arise during the electrooxidation of glycerol (or other small alcohols) on a platinum surface. Consequently, special attention is given to the thorough analysis of the CO band signal recorded throughout both consecutive step-potential scans, focusing on the dependence of its behavior on the electrolyte anions.

Firstly, it should be mentioned that the signal response of the in situ FTIR technique is notably influenced by the thin layer's thickness and is intrinsically related to these particular experimental conditions. In this case, we performed two consecutive scans. During the second scan, the surface of the electrode was already modified by CO, and other adsorbates formed in the first scan. Additionally, products generated during the first scan, including partially oxidized soluble species, remained dissolved in the thin layer, which could potentially influence the spectral features observed in the second scan.

While a direct comparison is feasible only in a semi-quantitative way due to the non-direct comparability of band intensities between the anions, the result of the integration of the different bands (Fig. S3) indicates that the ratio of the partial oxidation products follows the trend HClO<sub>4</sub>>H<sub>2</sub>SO<sub>4</sub>>H<sub>3</sub>PO<sub>4</sub>, that is, the ratio partial oxidation products diminishes with the anion adsorption strength. A more quantitative analysis can be performed by analyzing the ratio of the CO band

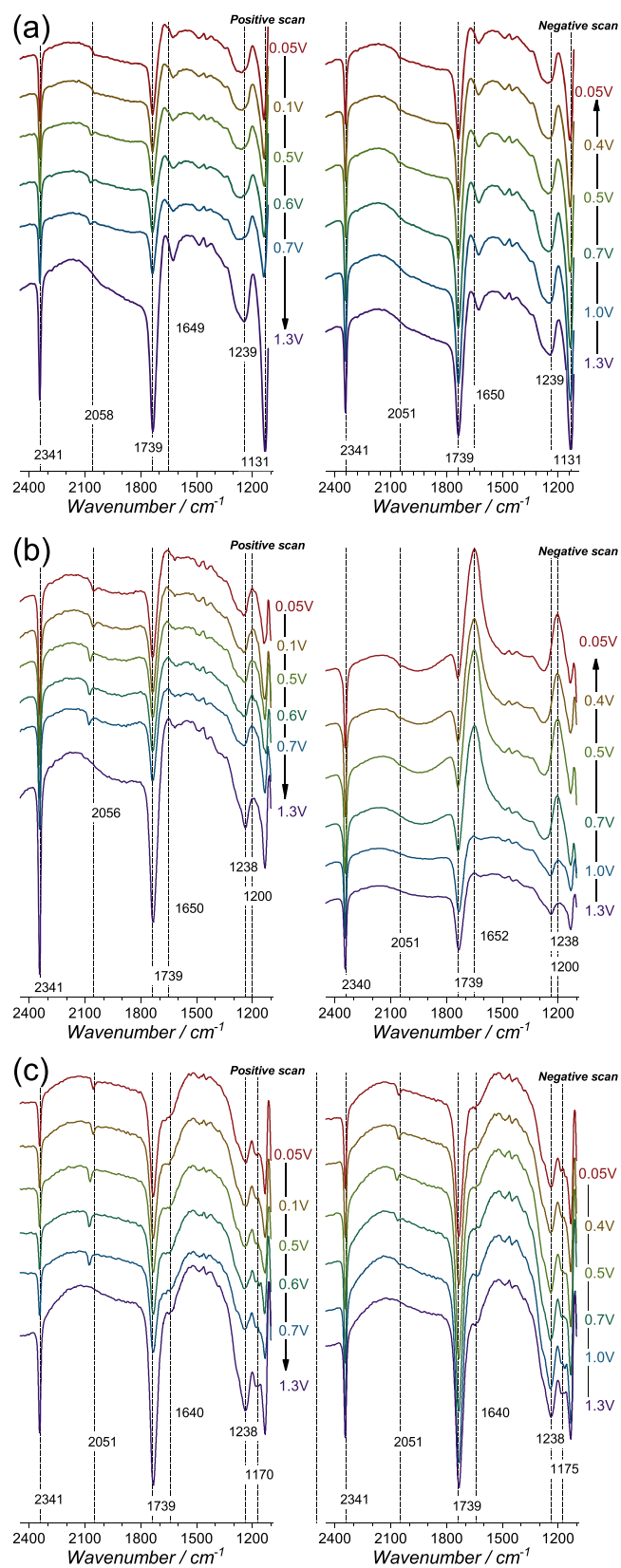


**Fig. 3.** Series of *in situ* FTIR spectra of Pt recorded (2nd scan) for consecutive potential steps cycling: positive and negative scan directions in 0.5 mol L<sup>-1</sup> glycerol + 1.0 mol L<sup>-1</sup> HClO<sub>4</sub>, H<sub>2</sub>SO<sub>4</sub> and H<sub>3</sub>PO<sub>4</sub>. Sample spectra were collected at the indicated potentials.

intensity to that corresponding to the  $\text{CO}_2$  band. This approach can offer valuable insights into the electrochemical processes occurring at the electrode-electrolyte interface. Fig. 4 illustrates the integrated band intensity ratio of adsorbed CO and  $\text{CO}_2$  ( $R_{\text{CO}}/R_{\text{CO}_2}$ ) at various potentials for different anions.

The absence of a bipolar band around  $2050\text{ cm}^{-1}$  indicates that linearly bonded CO was not formed at the reference potential across all studied electrolyte compositions. All FTIR experiments take into account that the protocol of polarizing the electrode at  $0.050\text{ V}$  was applied in all FTIR experiments to avoid the formation of parallel reactions such as CO appearance at low potential.

This observation is consistent with prior research wherein the authors examined glycerol electrooxidation reaction on Pt surfaces in  $\text{H}_2\text{SO}_4$  solution [20]. The  $\text{CO}_L$  band only emerges during the negative scan direction at  $0.7\text{ V}$  in the first scan, implying that CO is only formed from the oxidation products of glycerol. As the potential is decreased from that point, CO will progressively accumulate on the surface and is visible until the electrode reaches a potential of  $0.6\text{ V}$  in the subsequent positive scan. This potential coincides with the onset of the electrochemical oxidation of glycerol. (See Fig. 1). As the potential becomes more positive, the oxidation rate of  $\text{CO}_{\text{ads}}$  is favored in comparison to the cleavage of the C–C bond. Consequently,  $\text{CO}_{\text{ads}}$  is readily oxidized, leading to the disappearance of the  $\text{CO}_L$  band signal within the potential window of  $0.7$  to  $1.3\text{ V}$ . It is reasonable to propose that within this potential range, glycerol molecules and other soluble partial products generated from its oxidation will compete with adsorbed CO for Pt sites.

It is important to highlight that the relative intensity of the  $\text{CO}_L$  band increases with the anion strength, indicating that the oxidation of

glycerol molecules and the subsequent formation of adsorbed molecules are strongly influenced by the nature of the anions. Consequently, once  $\text{CO}_{\text{ads}}$  is formed, its oxidation and the concomitant reactivation of the surface catalytic sites are dependent on the presence of platinum  $\text{OH}_{\text{ads}}$  species. These species react with CO to yield  $\text{CO}_2$ , following a Langmuir-Hinshelwood (LH) mechanism. However, in the potential region where the CO oxidation reaction occurs (significantly higher than the potential of zero total charge for this surface) [37,38], the competitive adsorption of anions and/or OH species for Pt-free sites becomes a critical factor. In this context, the stronger the anion adsorption strength, the more challenging it becomes for OH species to form, inhibiting its formation and resulting in a relatively slower reaction rate of CO oxidation, as reflected in the current density profile in Fig. 1. Similarly, Angelucci et al. [1] have reported that the CO electrooxidation kinetic is strongly affected by the electrolyte anion present in the solution electrolyte.

The greater amount of adsorbed CO detected by FTIR cannot necessarily be linked to an ease of C–C bond cleavage but must be considered as well as the extent of its remaining on the electrode surface, about the overall electrooxidation kinetics of the solution reactants. In this way, another factor that should also be considered when analyzing the differences in the overall reaction rates is the adsorption of glycerol and other reactive products, such as carboxylic acids. Close to the electrode surface, these reactive species are present at high concentrations and can readily adsorb by competing for free Pt sites. Likewise, as previously discussed in the preceding paragraphs, the role of anion strength adsorption should also inhibit this process, thereby leading to the differences observed in the reaction rates. However, at present, it is not possible to definitively determine which pathway primarily

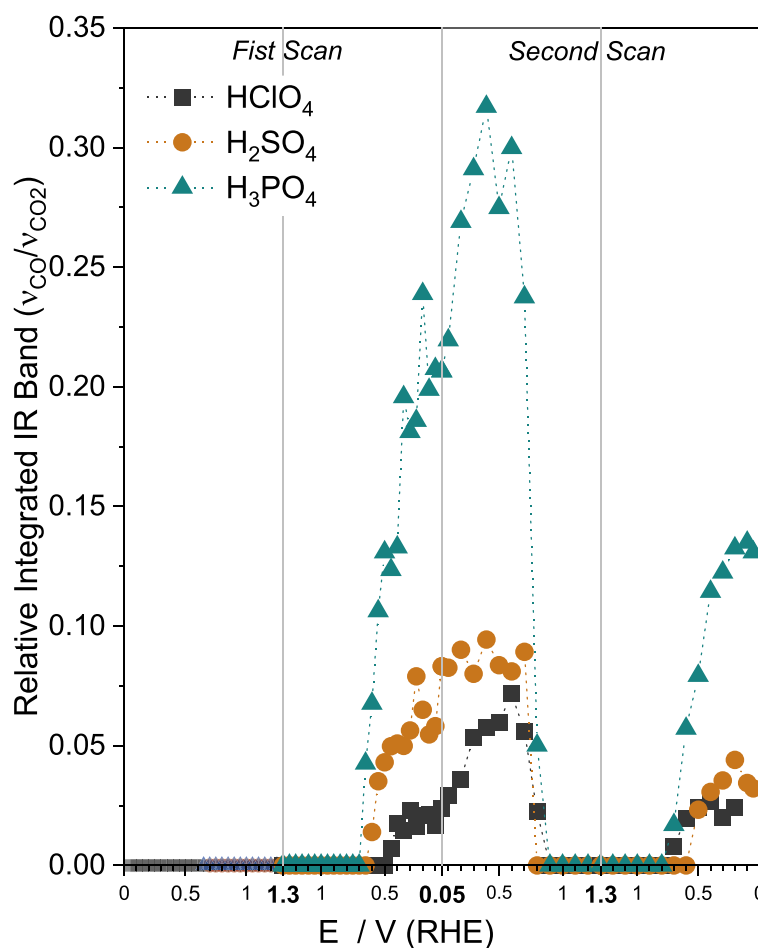


Fig. 4. Potential dependent integrated band intensities of ratio between carbon monoxide species ( $\text{CO}_L$ ) and carbon dioxide, ( $\text{CO}_2$ ) from FTIR spectra for GEOR on Pt electrode in 3 different acids electrolytes, namely  $\text{HClO}_4$ ,  $\text{H}_2\text{SO}_4$ , and  $\text{H}_3\text{PO}_4$ . (Data obtained from Fig. S2): Dotted lines connecting the data are just for visual aid.

contributes to the observed differences in the overall reaction rates among the three studied electrolytes. Both factors likely play a role in these variations.

In a broader context, the mechanism underlying the GEOR can be rationalized through the interplay of three distinct factors: (i) the activity facilitating the oxidation of glycerol to glyceraldehyde/glyceric acid in the presence of adsorbed anions, (ii) the capability to cleave the C–C bond, yielding CO, and (iii) the ability in adsorbing OH to facilitate the oxidation of CO to CO<sub>2</sub>. The highest catalytic activity is discerned on the surface that optimally combines these factors.

To gather additional insights about the previous discussion, oscillatory studies on the presence of the three anions were performed.

### 3.2. Oscillatory electrooxidation of glycerol on platinum

The platinum-catalyzed oxidation of glycerol in an acidic environment is prone to potential instability, primarily due to the intense competition between glycerol molecules and their intermediates for catalytic sites [16,23]. In order to better understand the effect of ions on glycerol oxidation, the same experimental method used by Sitta et al. [39] in the study of the effect of cations on the emergence of potential oscillations during the oxidation of ethylene glycol to platinum was employed. Fig. 5 shows, on the left column, the potentiodynamic curve registered for GEOR at 0.01 V s<sup>-1</sup> with different external resistances ( $R_{\text{ext}}$ ) between the working and reference electrodes, in the presence of the three studied anions. The potentiodynamic curves with no external ohmic resistance applied ( $R_{\text{ext}} = 0$ ) are also presented, which are the

same current density profile responses already shown in Fig. 1. It is important to highlight those high values of  $R_{\text{ext}}$  lead to a significant shift between the real electrode potential ( $\varphi$ ) and the applied circuit potential ( $E$ ). Thus,  $\varphi = E - I R_{\text{ext}}$ ; where  $I$  is the value of the current flowing in the circuit. Curves of the current density vs.  $E$  and  $\varphi$  are shown in the left and right columns of Fig. 5, respectively. These curves show the emergence of dynamic instabilities for GEOR in the three electrolytes with different values of  $R_{\text{ext}}$ . The extent of potential oscillations depends inversely on the strength of anion adsorption, spanning from 0.45 - 0.70 V for HClO<sub>4</sub> to 0.38 - 0.80 V for H<sub>3</sub>PO<sub>4</sub>.

Following our initial exploratory approach concerning the emergence of the oscillatory processes, a further in-depth analysis of the dynamics under potentiostatic conditions was carried out. To make the comparison between the three different systems here studied, it is necessary to consider and evaluate the potential window where the dynamic instabilities are observed during the linear potential sweep (See Fig. 5). Using a modified protocol from Ref. [40], the potential applied to the electrochemical system containing different anions was determined by the following equation:

$$E_N = \frac{E_{\text{osc}} - E_{\text{osc},i}}{E_{\text{osc},f} - E_{\text{osc},i}}$$

where  $E_{\text{osc}}$  is the applied potential, and  $E_{\text{osc},i}$  and  $E_{\text{osc},f}$  are the initial and final potentials of the oscillation region, as measured by the linear potential sweep shown in Fig. 5(a1-c1). Then, the potential for which  $E_N = 0.5$ , that is, the central point of the oscillation region, was selected. The current transient for this potential was recorded and the value of  $\varphi$  for

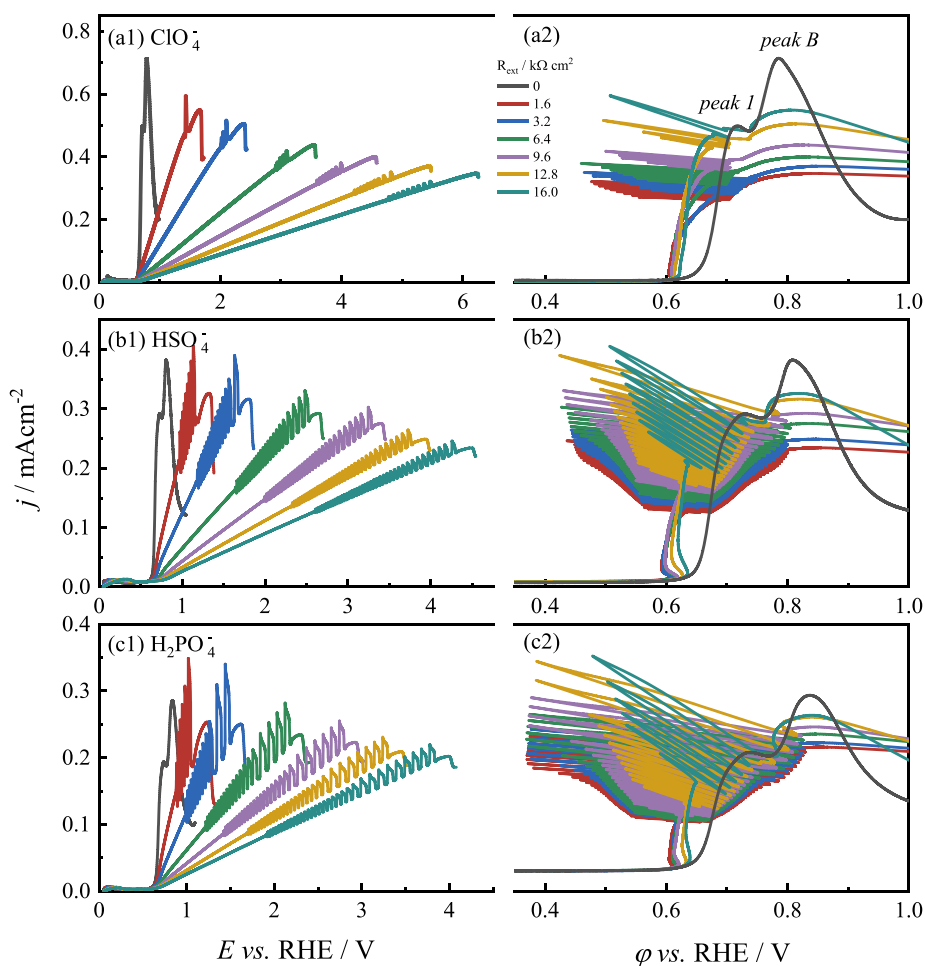


**Fig. 5.** Linear sweep at 0.01 V s<sup>-1</sup> during glycerol electrooxidation in 1 mol L<sup>-1</sup> of (a) HClO<sub>4</sub>, (b) H<sub>2</sub>SO<sub>4</sub>, and (c) H<sub>3</sub>PO<sub>4</sub> with different external resistors. Right panels (1) and left panels (2) show curves of  $j$  vs  $E$  and  $j$  vs  $\varphi$ , respectively.

each point was calculated.

Fig. 6 shows the stable interval region in the oscillatory curves of  $\varphi$  vs. time for  $R_{\text{ext}} = 9.6 \text{ k}\Omega \text{ cm}^2$  and  $E_{\text{osc}} = 3.80, 2.64$  and  $2.00 \text{ V}$ , in  $1 \text{ mol L}^{-1} \text{ HClO}_4$ ,  $\text{H}_2\text{SO}_4$ , and  $\text{H}_3\text{PO}_4$ , respectively (The complete series are presented in Fig.S4). In all cases, 1-period oscillations are observed and the anion adsorption strength affects the general waveform of the oscillatory potential cycle. The potential oscillations region ( $\varphi$ ) occurs in the same region where  $\text{CO}_{\text{ad}}$  formation takes place and the maximum potential of the oscillations (oscillation peak) is close to the  $\text{CO}_{\text{ad}}$  oxidation potential, as confirmed by in situ FTIR (Fig. 4). Another point to report is that the short duration of oscillations for the system in the presence of  $\text{HClO}_4$  may be assigned to slower kinetics in the formation of  $\text{CO}_{\text{ads}}$  compared to systems with  $\text{H}_2\text{SO}_4$  or  $\text{H}_3\text{PO}_4$ , as indicated by the  $\text{CO}_{\text{ads}}$  coverage observed in the FTIR experiments (SI – S2).

These findings are consistent with those reported by Melle et al. [23], where the authors demonstrated a direct correlation between potential instability and  $\text{CO}_{\text{ads}}$  formation on the electrode surface. However, under experimental conditions where  $\text{CO}_{\text{ads}}$  formation either occurs with minimal intensity or is virtually nonexistent, potential instabilities are mitigated. In the case of  $\text{HClO}_4$ , the cycle modulation initiates at ca.  $0.58 \text{ V}$ , with a gradual increase in electrode potential up to  $0.70 \text{ V}$ . However, for the other two anions where specific adsorption takes place, the cycle modulation rises at  $0.50 \text{ V}$ , accompanied by a sharp increase in potential up to  $0.7 \text{ V}$ . In other words, the oscillatory behavior in the oxidation of glycerol is linked to surface poisoning. Specifically, a less poisoned surface results in fewer oscillations, as observed by Melle et al. [23]. Accordingly, our oscillatory experiments reveal that in  $\text{HClO}_4$ , the system exhibits fewer oscillations, consistent with the formation of less CO in contrast to the other two coordinating anions. This observation aligns with our FTIR results and provides robust evidence for the anion-dependent reaction pathways.

To gain a deeper understanding of the described process, it is essential to consider that under the oscillatory regime, a minimum of

two elementary steps collaborate in generating the observed regular oscillations. Initially, a process dominated by hindering the surface with strongly adsorbed species defines the transition from slow activity (at low potentials) to a passive state ( $> 0.6 \text{ V}$ ). In this passive state,  $\text{OH}_{\text{ads}}$  species can form and subsequently oxidize the adsorbed poisoning species, undergoing an electrooxidative cleaning of the electrode surface resulting in a sharp drop in potential.

From a mechanistic perspective, it is worth noting the significant correspondence between the potential window in which the oscillations occur, and the region between the onset potential and *peak 1* recorded during the positive scan direction in the voltammetric profiles (Fig. 1). The potential window of the oscillations is notably correlated with the accumulation and subsequent oxidation of  $\text{CO}_{\text{ads}}$  observed in the FTIR results. In this way, it is reasonable to conclude that the primary poisoning species related to the slow step can be attributed to  $\text{CO}_{\text{ads}}$ .

However, although not fully demonstrated here by spectroscopic studies, the effect of the nature of the anions in the  $\text{OH}_{\text{ads}}$  species formation should be considered. It is worth noting that the oscillations occur within a potential range where the formation of  $\text{OH}_{\text{ads}}$  is favored, and the Pt electrode surface is partially covered. Additionally, in this same potential window, the extent of  $\text{OH}_{\text{ads}}$  formation is influenced by the anions' affinity to the metal surface and competition is established between water and the anions for available Pt sites [22,41]. When specific anion adsorption occurs, the  $\text{OH}_{\text{ads}}$  formation becomes more difficult than for non-coordinated anion (namely  $\text{HClO}_4$ ) and subsequently slows down the surface cleaning process through  $\text{CO}_{\text{ads}}$  oxidation. This interpretation helps explain the lower frequency of oscillation in the  $\text{H}_3\text{PO}_4$  electrolyte compared to  $\text{H}_2\text{SO}_4$  and the lower potential amplitude for  $\text{HClO}_4$  oscillations. In this sense, Malkandi et al. [42] have reported that any anion that competes with the oxidative chemisorption of water at free sites on the electrode surface could induce oscillations in some concentration range. The authors showed that by replacing  $\text{HBF}_4$  with chloride or sulfate anions, oscillatory rise from CO

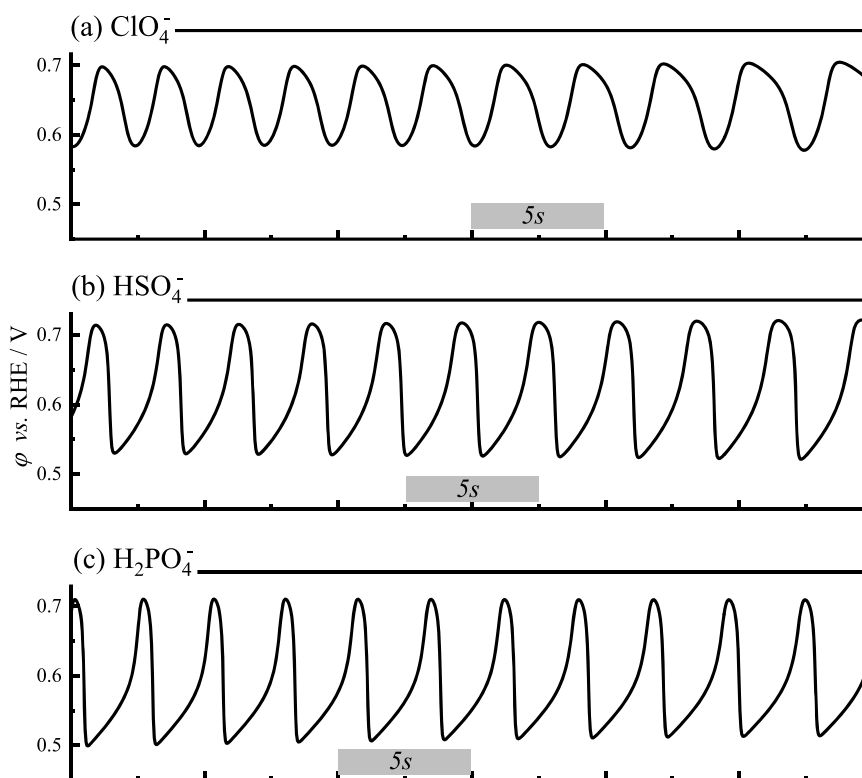


Fig. 6. Potentiostatic time series for GEOR in  $1.0 \text{ mol L}^{-1}$  of the following electrolytes: (a)  $\text{HClO}_4$ , (b)  $\text{H}_2\text{SO}_4$  (c)  $\text{H}_3\text{PO}_4$ , respectively, with  $R_{\text{ext}}$  ( $9.6 \text{ k}\Omega \text{ cm}^2$ ) corrected.



electrooxidation.

Finally, it is possible to conclude that different anions influence the electroactivity and selectivity of glycerol oxidation and therefore, the pathways may be affected. In the case of the lower strength of adsorption,  $\text{ClO}_4^-$  adsorption, the CO formation is less favored, probably due to glycerol adsorption on Pt that promotes the formation of species C3 type with carboxylic groups, through a direct reaction pathway, while strong interaction of anions ( $\text{HSO}_4^-$  and  $\text{H}_2\text{PO}_4^-$ ) the glycerol adsorbs producing more glyceraldehyde and, consequently, more CO [43].

#### 4. Conclusions

This study has provided a detailed exploration of the glycerol electrooxidation mechanism on platinum electrodes, emphasizing the crucial role played by the anion in the electrolyte composition. Our findings demonstrate that the nature of the anion significantly affects the electrooxidation process, with the strength of anion adsorption following the order  $\text{HClO}_4 < \text{H}_2\text{SO}_4 < \text{H}_3\text{PO}_4$ . This trend influences the rate of glycerol electrooxidation, primarily due to competitive adsorption phenomena where more strongly coordinating anions exhibit enhanced adsorption capabilities compared to perchlorate ions.

Through in situ FTIR spectroscopy, we identified three distinct bands corresponding to  $\nu(\text{C}=\text{O})$ ,  $\nu(\text{C-O})$ , and  $\nu(\text{CO}_2)$ , which provided valuable insights into the mechanism of glycerol electrooxidation. These results indicate a selectivity towards carboxylic acid formation and highlight the ability to cleave C-C bonds, leading to CO production. The intensity of the  $\text{CO}_L$  band increases with anion strength, underscoring the significant impact of anion nature on both the oxidation of glycerol molecules and the subsequent formation of adsorbed intermediates.

Additionally, the observed oscillatory responses and the distinct behavior of the CO band signal with varying anion strength revealed a complex interplay between anion adsorption and the electrooxidation mechanism. These findings suggest that different anions can induce unique GEOR pathways, providing a deeper understanding of the factors influencing electrochemical reactions on platinum electrodes.

#### CRediT authorship contribution statement

**Gabriel Melle:** Conceptualization, Methodology, Investigation, Writing – review & editing. **Juan M. Feliu:** Writing – review & editing. **Enrique Herrero:** Writing – review & editing. **Germano Tremiliosi-Filho:** Writing – review & editing. **Vinicius Del Colle:** Conceptualization, Methodology, Investigation, Writing – review & editing. **Camilo A. Angelucci:** Conceptualization, Methodology, Writing – review & editing.

#### Declaration of competing interest

The authors declare that they have no known competing financial interests or personal relationships that could have appeared to influence the work reported in this paper.

#### Acknowledgments

G.M., E.H., and J.F. gratefully acknowledge financial support from Ministerio de Ciencia e Innovación (Project PID2022-137350NB-I00). V. D.C. gratefully acknowledges financial support from FAPEAL and CNPq (process E:60030.0000002494/2022 and Grant N<sup>o</sup>. 312788/2022-3). G. T.F. (Grant N<sup>o</sup> 2019/22183-6) acknowledges the São Paulo State Research Foundation - Brazil (FAPESP) for financial support. G.T.F. (Grant N<sup>o</sup> 3134455/2021-0 and 408069-2022-8) acknowledges the Conselho Nacional de Desenvolvimento Científico e Tecnológico - Brazil (CNPq) for financial support. G.T.F. acknowledges the support of the RCGI – Research Centre for Gas Innovation, hosted by the University of São Paulo (USP) and sponsored by FAPESP (2020/15230-5) and Shell Brasil (CW410367), and the strategic importance of the support given by

ANP (Brazil's National Oil, Natural Gas, and Biofuels Agency) through the R&D levy regulation. C.A.A. gratefully acknowledges financial support from FAPESP through projects 2018/10292-2 and 2022/11345-8.

#### Supplementary materials

Supplementary material associated with this article can be found, in the online version, at [doi:10.1016/j.electacta.2024.144698](https://doi.org/10.1016/j.electacta.2024.144698).

#### References

- [1] C.A. Angelucci, F.C. Nart, E. Herrero, J.M. Feliu, Anion re-adsorption and displacement at platinum single crystal electrodes in CO-containing solutions, *Electrochem. Commun.* 9 (2007) 1113–1119, <https://doi.org/10.1016/j.elecom.2007.01.012>.
- [2] J.F. Gomes, C.A. Martins, M.J. Giz, G. Tremiliosi-Filho, G.A. Camara, Insights into the adsorption and electro-oxidation of glycerol: self-inhibition and concentration effects, *J. Catal.* 301 (2013) 154–161, <https://doi.org/10.1016/j.jcat.2013.02.007>.
- [3] F. Colmati, G. Tremiliosi-Filho, E.R. Gonzalez, A. Berná, E. Herrero, J.M. Feliu, Surface structure effects on the electrochemical oxidation of ethanol on platinum single crystal electrodes, *Faraday Discuss* 140 (2008) 379–397, <https://doi.org/10.1039/b802160k>.
- [4] C. Busó-Rogero, V. Grozovski, F.J. Vidal-Iglesias, J. Solla-Gullón, E. Herrero, J. M. Feliu, Surface structure and anion effects in the oxidation of ethanol on platinum nanoparticles, *J. Mater. Chem. A* 1 (2013) 7068, <https://doi.org/10.1039/c3ta10996h>.
- [5] J.V. Perales-Rondón, E. Herrero, J.M. Feliu, On the activation energy of the formic acid oxidation reaction on platinum electrodes, *J. Electroanal. Chem.* 742 (2015) 90–96, <https://doi.org/10.1016/j.jelechem.2015.02.003>.
- [6] N. Garcia-Araez, V. Climent, E. Herrero, J. Feliu, J. Lipkowski, Thermodynamic studies of bromide adsorption at the Pt(1 1 1) electrode surface perchloric acid solutions: comparison with other anions, *J. Electroanal. Chem.* 591 (2006) 149–158, <https://doi.org/10.1016/j.jelechem.2006.04.008>.
- [7] J.V. Perales-Rondón, E. Herrero, J.M. Feliu, Effects of the anion adsorption and pH on the formic acid oxidation reaction on Pt(111) electrodes, *Electrochim. Acta* 140 (2014) 511–517, <https://doi.org/10.1016/j.electacta.2014.06.057>.
- [8] E. Herrero, K. Franaszczuk, A. Wieckowski, Electrochemistry of methanol at low index crystal planes of platinum. An integrated voltammetric and chronoamperometric study, *J. Phys. Chem.* 98 (1994) 5074–5083, <https://doi.org/10.1021/j100070a022>.
- [9] R. Nagao, D.A. Cantane, F.H.B. Lima, H. Varela, Influence of anion adsorption on the parallel reaction pathways in the oscillatory electro-oxidation of methanol, *J. Phys. Chem. C* 117 (2013) 15098–15105, <https://doi.org/10.1021/jp4028047>.
- [10] R.N.S. Lima, J. Souza-garcia, C.A. Angelucci, Electrochemical surface-enhanced Raman spectroscopy (EC-SERS) Study of C3 polyalcohols oxidation catalyzed by a Ag roughened electrode with low platinum content, *J. Phys. Chem. C* 127 (2023) 16374–16384, <https://doi.org/10.1021/acs.jpcc.3c03039>.
- [11] T. Li, D.A. Harrington, An overview of glycerol electrooxidation mechanisms on Pt, Pd and Au, *ChemSusChem* 14 (2021) 1472–1495, <https://doi.org/10.1002/cssc.202002669>.
- [12] Y. Zhou, Y. Shen, J. Piao, Sustainable conversion of glycerol into value-added chemicals by selective electro-oxidation on Pt-based catalysts, *ChemElectroChem* 5 (2018) 1636–1643, <https://doi.org/10.1002/celec.201800309>.
- [13] C.A. Angelucci, J. Souza-Garcia, P.S. Fernández, P.V.B. Santiago, R.M.L. M. Sandrini, Glycerol electrooxidation on noble metal electrode surfaces. *Encycl. Interfacial Chem*, Elsevier, 2018, pp. 643–650, <https://doi.org/10.1016/B978-0-12-409547-2.13330-X>.
- [14] T. Iwasita, Electrocatalysis of methanol oxidation, *Electrochim. Acta.* 47 (2002) 3663–3674, [https://doi.org/10.1016/S0013-4686\(02\)00336-5](https://doi.org/10.1016/S0013-4686(02)00336-5).
- [15] M.E. Paulino, L.M.S. Nunes, E.R. Gonzalez, G. Tremiliosi-Filho, situ FTIR spectroscopic study of ethanol oxidation on Pt(111)/Rh/Sn surface, The anion effect, *Electrochem. Commun* 52 (2015) 85–88, <https://doi.org/10.1016/j.elecom.2014.12.025>.
- [16] V. Del Colle, G. Melle, B.A.F. Previdello, J.M. Feliu, H. Varela, G. Tremiliosi-Filho, The effect of Pt surface orientation on the oscillatory electro-oxidation of glycerol, *J. Electroanal. Chem.* 926 (2022) 116934, <https://doi.org/10.1016/j.jelechem.2022.116934>.
- [17] N.M. Markovic, C.A. Lucas, A. Rodes, V. Stamenkovic, P.N. Ross, Surface electrochemistry of CO on Pt(1 1 1): anion effects, *Surf. Sci.* 499 (2002). <http://www.scopus.com/inward/record.url?eid=2-s2.0-0036499837&partneRid=40&md5=7284d0c3b3b79622c1fd65706649072a>.
- [18] G. Melle, F. Scholten, J.M. Feliu, E. Herrero, B.R. Cuenya, R.M. Arán-Ais, Elucidating interfacial parameters of platinum–palladium bulk alloy single crystals, *J. Mater. Chem. A* 12 (2024) 15321–15333, <https://doi.org/10.1039/D4TA01771D>.
- [19] P.S. Fernández, C.A. Martins, C.A. Angelucci, J.F. Gomes, G.A. Camara, M. E. Martins, G. Tremiliosi-Filho, Evidence for independent glycerol electrooxidation behavior on different ordered domains of polycrystalline platinum, *ChemElectroChem* 2 (2015) 263–268, <https://doi.org/10.1002/celec.201402291>.
- [20] P.S. Fernández, J. Fernandes Gomes, C.A. Angelucci, P. Tereshchuk, C.A. Martins, G.A. Camara, M.E. Martins, J.L.F. Da Silva, G. Tremiliosi-Filho, Establishing a link

- between well-ordered Pt(100) surfaces and real systems: how do random superficial defects influence the electro-oxidation of glycerol? ACS Catal 5 (2015) 4227–4236, <https://doi.org/10.1021/acscatal.5b00451>.
- [21] J. Mostany, P. Martínez, V. Climent, E. Herrero, J.M. Feliu, Thermodynamic studies of phosphate adsorption on Pt(1 1 1) electrode surfaces in perchloric acid solutions, *Electrochim. Acta* 54 (2009) 5836–5843. <http://www.scopus.com/inward/record.url?eid=2-s2.0-67649224016&partnerID=40&md5=f7ac9b7a19183be91a7d47a62f5b573a>.
- [22] E. Herrero, J. Mostany, J.M. Feliu, J. Lipkowski, Thermodynamic studies of anion adsorption at the Pt(111) electrode surface in sulfuric acid solutions, *J. Electroanal. Chem.* 534 (2002) 79–89. <http://www.scopus.com/inward/record.url?eid=2-s2.0-0037019843&partnerID=40&md5=41da72194875444cc7fe14683f0c4b55>.
- [23] G.B. Melle, E.G. Machado, L.H. Mascaró, E. Sitta, Effect of mass transport on the glycerol electro-oxidation, *Electrochim. Acta* 296 (2019) 972–979, <https://doi.org/10.1016/j.electacta.2018.11.085>.
- [24] M.F. Cabral, R. Nagao, E. Sitta, M. Eiswirth, H. Varela, Mechanistic aspects of the linear stabilization of non-stationary electrochemical oscillations, *Phys. Chem. Chem. Phys.* 15 (2013) 1437–1442, <https://doi.org/10.1039/C2CP42890C>.
- [25] M.G. de Oliveira, G.B. Melle, R.L. Romano, H. Varela, The impact of water concentration on the electro-oxidation of formic acid on platinum, *J. Electrochem. Soc.* 169 (2022) 026514, <https://doi.org/10.1149/1945-7111/ac5060>.
- [26] G.B. Melle, F.W. Hartl, H. Varela, E. Sitta, The effect of solution pH on the oscillatory electro-oxidation of methanol, *J. Electroanal. Chem.* 826 (2018) 164–169, <https://doi.org/10.1016/j.jelechem.2018.08.033>.
- [27] R.M. Arán-Ais, E. Herrero, J.M. Feliu, The breaking of the CC bond in ethylene glycol oxidation at the Pt(111) electrode and its vicinal surfaces, *Electrochem. Commun.* 45 (2014) 40–43, <https://doi.org/10.1016/j.elecom.2014.05.008>.
- [28] L.F. Sallum, A. Mota-Lima, E.R. Gonzalez, Galvano- and potentiodynamic studies during ethanol electro-oxidation reaction in acid vs. alkaline media: energy dissipation and blocking nature of potassium, *Electrochim. Acta* 293 (2019) 247–259, <https://doi.org/10.1016/j.electacta.2018.09.118>.
- [29] P.S. Fernández, P. Tereshchuk, C.A. Angelucci, J.F. Gomes, A.C. Garcia, C. A. Martins, G.A. Camara, M.E. Martins, J.L.F. Da Silva, G. Tremiliosi-Filho, How do random superficial defects influence the electro-oxidation of glycerol on Pt(111) surfaces? *Phys. Chem. Chem. Phys.* 18 (2016) 25582–25591, <https://doi.org/10.1039/C6CP04768H>.
- [30] G. Melle, M.B.C. de Souza, P.V.B. Santiago, P.G. Corradini, L.H. Mascaró, P. S. Fernández, E. Sitta, Glycerol electro-oxidation at Pt in alkaline media: influence of mass transport and cations, *Electrochim. Acta* 398 (2021) 139318, <https://doi.org/10.1016/j.electacta.2021.139318>.
- [31] J. Souza-Garcia, C.A. Angelucci, The role of anions in single crystal platinum cyclic voltammograms, *Quim. Nova* 38 (2015) 669–678, <https://doi.org/10.5935/0100-4042.20150048>.
- [32] V. Del Colle, L.M.S.M.S. Nunes, C.A.A. Angelucci, J.M.M. Feliu, G. Tremiliosi-Filho, The influence of stepped Pt[n(111)×(110)] electrodes towards glycerol electrooxidation: electrochemical and FTIR studies, *Electrochim. Acta* 346 (2020) 136187, <https://doi.org/10.1016/j.electacta.2020.136187>.
- [33] P.V.B. Santiago, R.A.G. Oliveira, J.M. Roquette, N. Akiba, I. Gaubeur, C. A. Angelucci, J. Souza-Garcia, J.M. Feliu, Oxide formation as probe to investigate the competition between water and alcohol molecules for OH species adsorbed on platinum, *Electrochim. Acta* 317 (2019) 694–700. <https://linkinghub.elsevier.com/retrieve/pii/S0013468619311806> (accessed June 17, 2019).
- [34] Y. Kwon, M.T.M. Koper, Combining voltammetry with HPLC: application to electro-oxidation of glycerol, *Anal. Chem.* 82 (2010) 5420–5424, <https://doi.org/10.1021/ac101058t>.
- [35] J. Schnaidt, M. Heinen, D. Denot, Z. Jusys, R. Jürgen Behm, Electrooxidation of glycerol studied by combined in situ IR spectroscopy and online mass spectrometry under continuous flow conditions, *J. Electroanal. Chem.* 661 (2011) 250–264, <https://doi.org/10.1016/j.jelechem.2011.08.011>.
- [36] R.N.S. Lima, V. Del, G. Tremiliosi-filho, C.A. Angelucci, Electrochimica acta unveiling the effect of Pt addition on Ag /C catalyst for enhanced glycerol electrooxidation, *Electrochim. Acta* (2024) 144181, <https://doi.org/10.1016/j.electacta.2024.144181>.
- [37] J. Souza-Garcia, C.A. Angelucci, V. Climent, J.M. Feliu, Electrochemical features of Pt(S)[n(110)×(100)] surfaces in acidic media, *Electrochem. Commun.* 34 (2013) 291–294, <https://doi.org/10.1016/j.elecom.2013.07.007>.
- [38] V. Climent, N. García-Araez, E. Herrero, J. Feliu, Potential of zero total charge of platinum single crystals: a local approach to stepped surfaces vicinal to Pt(111), *Russ. J. Electrochem.* 42 (2006) 1145–1160, <https://doi.org/10.1134/S1023193506110012>.
- [39] E. Sitta, R. Nagao, I.Z.L.Z. Kiss, H. Varela, Impact of the alkali cation on the oscillatory electro-oxidation of ethylene glycol on platinum, *J. Phys. Chem. C* 119 (2015) 1464–1472, <https://doi.org/10.1021/jp5105505>.
- [40] R. Nagao, I.R. Epstein, E.R. Gonzalez, H. Varela, Temperature (over)compensation in an oscillatory surface reaction, *J. Phys. Chem. A* 112 (2008) 4617–4624, <https://doi.org/10.1021/jp801361j>.
- [41] M. Weber, F.C. Nart, I.R. De Moraes, T. Iwasita, Adsorption of phosphate species on Pt(111) and Pt(100) as studied by in situ FTIR spectroscopy, *J. Phys. Chem.* 100 (1996) 19933–19938. <http://www.scopus.com/inward/record.url?eid=2-s2.0-33748389430&partnerID=40&md5=745e9df0a93cc9b713dc1c7bc969237c>.
- [42] S. Malkhandi, A. Bonnefont, K. Krischer, Strictly potentiostatic current oscillations during bulk CO electro-oxidation on platinum in the presence of inhibiting anions, *Electrochem. Commun.* 7 (2005) 710–716, <https://doi.org/10.1016/j.elecom.2005.04.022>.
- [43] A.C. Garcia, M.J. Kolb, C. van Nierop y Sanchez, J. Vos, Y.Y. Birdja, Y. Kwon, G. Tremiliosi-Filho, M.T.M.M. Koper, Strong impact of platinum surface structure on primary and secondary alcohol oxidation during electro-oxidation of glycerol, *ACS Catal.* 6 (2016) 4491–4500, <https://doi.org/10.1021/acscatal.6b00709>.